Thermogravimetric Study of the Ln_2O_3–Co–Co_2O_3 System

III. Ln = Pr, Sm, Eu, and Tb

KENZO KITAYAMA

Department of Chemistry, Faculty of Science, Tokyo Institute of Technology, Ookayama, Meguro-ku, Tokyo 152

Phase equilibria in the system Ln_2O_3–Co–Co_2O_3 (Ln = Pr, Sm, Eu, and Tb) at 1200°C were studied at oxygen partial pressure ranging from 1 to 10^{-12} atm O_2. "Pr_2CoO_4," $PrCoO_3$, and $Pr_4Co_3O_{10}$ are stable ternary compounds in the Pr_2O_3–Co–Co_2O_3 system, while only $LnCoO_3$-type compound is stable in the other systems. The standard Gibbs energies ($\Delta G°$) of reactions appearing in the systems were also determined from the oxygen partial pressures in equilibrium with three solid phases. $\Delta G°$ values for a reaction $\frac{1}{2}Ln_2O_3$ + CoO + $\frac{1}{4}O_2$ = $LnCoO_3$ fit well with the linear $\Delta G°$ vs ionic radius relation reported previously. © 1988 Academic Press, Inc.

In the previous studies (*1, 2*) Ln_2O_3–Co–Co_2O_3 (Ln = La, Nd, and Gd) was studied at 1200°C at oxygen partial pressures ranging from 1 to 10^{-12} atm O_2. In those systems, La_2CoO_4, $La_4Co_3O_{10}$, $LaCoO_3$, $Nd_4Co_3O_{10}$, $NdCoO_3$, and $GdCoO_3$ were stable ternary compounds, and those systems were classified into three types based upon the stable ternary compounds (*2*). Also the Gibbs energies of reactions which appear in the systems were determined, and the relationship between Gibbs energies for a common reaction, $\frac{1}{2}Ln_2O_3$ + CoO + $\frac{1}{4}O_2$ = $LnCoO_3$, and the ionic radius of lanthanoid with 12 coordination was linear (*2*).

In this paper Pr_2O_3, Sm_2O_3, Eu_2O_3, and Tb_2O_3 are chosen as Ln_2O_3.

$MCoO_3$ (M = La–Ho, Y) was prepared by adding Na_2CO_3 to solutions containing $M(NO_3)_3$ and Co-nitrate to coprecipitate the oxides and then by calcining the oxides at 700°C (*3*). $LaCoO_3$ is hexagonal whereas the other $MCoO_3$ compounds are or-

thorhombic. Ln_2CoO_4 and $LnCoO_3$ (Ln = La–Sm, Gd, Dy, Er, Yb) were prepared in a high-temperature imaging furnace (*4*). The oxygen pressure range which can be used with this technique (8×10^{-6}–200 atm) makes it possible to attain the II and III oxidation states of Co. Demazeau *et al.* (*5*) reported that $TCoO_3$ (T = Y, La–Lu) had been prepared under high oxygen pressure. $LaCoO_3$ is trigonal and $NdCoO_3$ is pseudo-tetragonal with orthorhombic symmetry and $GdFeO_3$-type structure as found in the following $TCoO_3$ phases.

Sm_2CoO_4 was prepared at a high temperature of 2000°C with a mixture of Sm_2O_3/CoO = 1 mole ratio under oxygen atmosphere, and lattice constants were measured with a single crystal (*6*). Pr_2CoO_4 was prepared under an atmosphere of N_2 in a temperature interval from 700 to 1200°C and its lattice constants were determined (*7*).

The compound $Pr_4Co_3O_{10}$, with tetrago-

nal structure and lattice constants $a = 5.39 \pm 0.05$, $c = 27.36 \pm 0.04$ Å, was prepared at 1100°C under partial pressure of 10^{-4} atm by Cherepanov et al. (8). Electromotive force (emf) measurement was used to determine thermodynamic characteristics.

Kropanov et al. (9) reported on the temperature dependence of the dissociation pressure of $LnCoO_3$ (Ln = Sm–Ho) into Ln_2O_3, CoO and O_2 at 800–1200°C by emf measurement. The Ln–Co–O phase diagrams were roughly constructed at 1273°K. The only ternary compound formed under the conditions of the study is $LnCoO_3$ with perovskite structure.

As summarized above, many researchers seem to be interested in compounds and very little work regarding phase equilibria has been performed.

The objectives of the present study were (1) to establish the detailed phase equilibria in these systems at 1200°C as a function of the oxygen partial pressure; (2) to calculate the thermochemical properties based upon the phase equilibria; (3) to ascertain in the Ln–Co–O system whether the phase diagram pattern would change with different lanthanoid elements; and (4) to determine whether a linear relationship between the Gibbs energy of reaction and lanthanoid ionic radius exists and is similar to that observed in the Ln–Fe–O (10) and Ln–V–O (11) systems.

Experimental

Analytical-grade Pr_6O_{11} (99.9%), Sm_2O_3 (99.9%), Eu_2O_3 (99.9%), Tb_4O_7 (99.9%), and CoO (99.9%) were used as starting materials. Recently, the oxygen partial pressure ranges in which Pr_2O_3 and Tb_2O_3 are stable were determined at 1000, 1100, and 1200°C (12). According to the results, Pr_6O_{11} and Tb_4O_7 are stable in the oxygen partial pressure higher than $10^{-0.70}$ and $10^{-1.75}$, respectively. Pr_6O_{11} and Tb_4O_7 were reduced to Pr_2O_3 and Tb_2O_3 at 1200°C in the

oxygen partial pressure of 10^{-10} atm for 5 hr (11). Hexagonal, light green Pr_2O_3 and white Tb_2O_3 with C-form were confirmed by the powder X-ray diffraction method (13, 14) and the compositions were determined to be $Pr_2O_{3.00}$ and $Tb_2O_{3.00}$ by EDTA titration. Sm_2O_3, Eu_2O_3, and CoO were preliminarily dried at 1200°C in air. Mixtures with desired molar ratios of Ln_2O_3/CoO were obtained by mixing the calculated amounts of constituent binary oxides thoroughly in an agate mortar. The mixtures thus obtained were heated at 1200°C several times during the intermediate mixing and were treated by the same procedures as those described previously (15).

The apparatus and means for controlling the oxygen partial pressures and keeping a constant temperature, the method of thermogravimetry, and the criterion for the establishment of equilibrium are the same as those described previously (15, 16).

X-ray powder analysis, employing Ni-filtered $CuK\alpha$ radiation from the compounds in the Pr–Co–O, Sm–Co–O, and Tb–Co–O systems, and Mn-filtered $FeK\alpha$ radiation for the compounds in the Eu–Co–O system, was used to characterize the phases present in the quenched samples. Lattice constants were also determined by the X-ray powder method with a slow scanning speed of 0.5° 2θ/min. A standard specimen of external silicon was used as 2θ calibrant. Mixtures of CO_2 and H_2 or CO_2 and O_2 were used to obtain the required oxygen partial pressure. The actual oxygen partial pressures were measured by means of a soid electrolytic cell, $(ZrO_2)_{0.85}(CaO)_{0.15}$ (17).

Results and Discussion

(1) Phase Equilibria

Pr_2O_3–Co–Co_2O_3 system. Eight mixtures with Pr_2O_3/CoO mole ratios of 6/4, 5.5/4.5, 4.75/5.25, 4.4/5.6, 4/6, 3/5, 3/7, and 2/8 were prepared to use in thermogravimetry. In
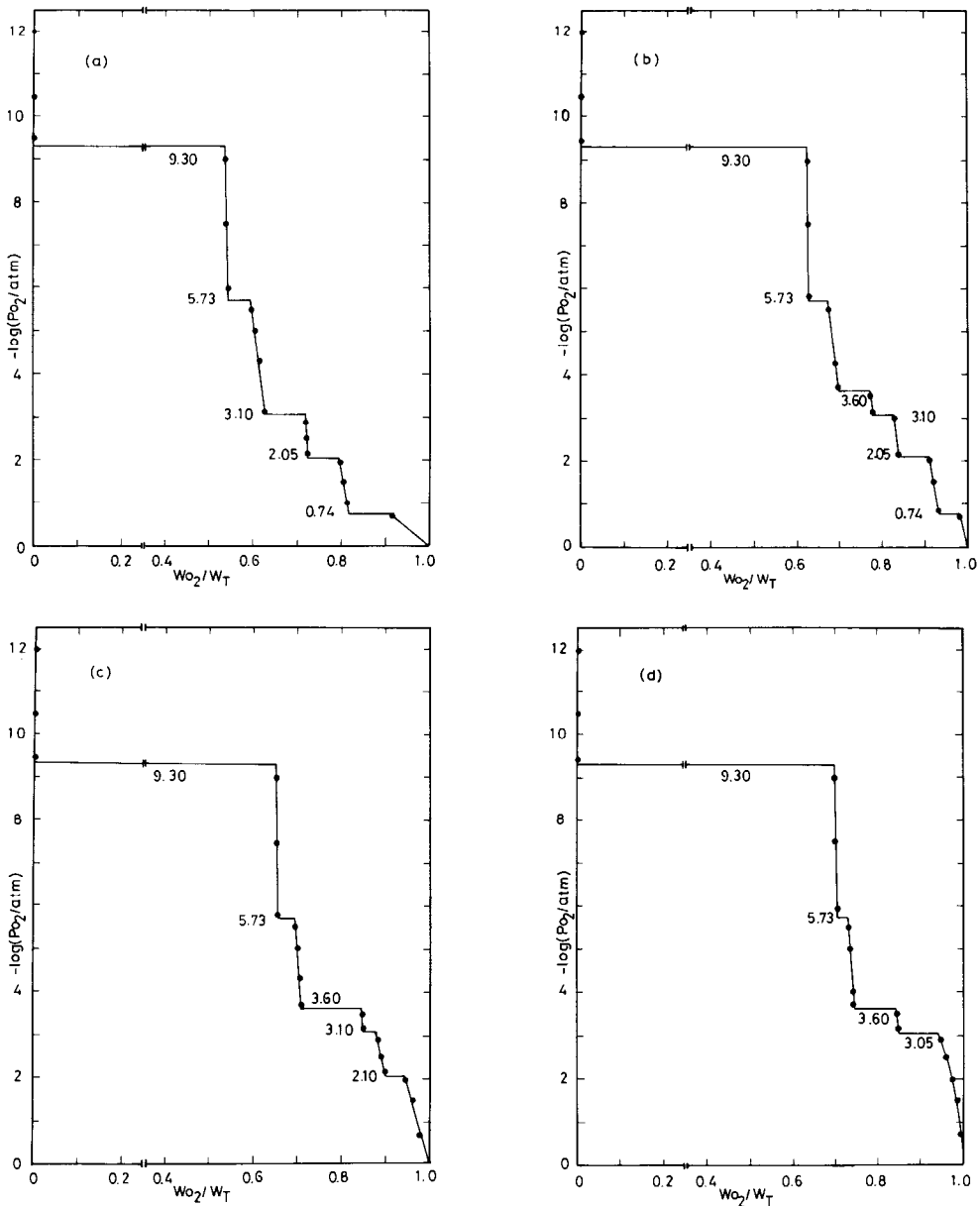
FIG. 1. The relationships between $-\log(P_{O_2}/\mathrm{atm})$ and the weight change, W_{O_2}/W_T, of samples in the Pr system. (a) $Pr_2O_3/CoO = 6/4$, (b) $Pr_2O_3/CoO = 4.4/5.6$, (c) $Pr_2O_3/CoO = 3/5$, (d) $Pr_2O_3/CoO = 3/7$.

Fig. 1 the relationships between the oxygen partial pressure, $-\log(P_{O_2}/\mathrm{atm})$, on the ordinate and the weight change, W_{O_2}/W_T, on the abscissa are shown for four representative samples, (a) 6/4, (b) 4.4/5.6, (c) 3/5, and (d) 3/7. W_{O_2} is the weight increase of the samples relative to the reference weight at $\log P_{O_2} = -12.00$, at which Pr_2O_3 and Co-metal coexists, and W_T is the total weight gain from the reference weight to the

weight at 1 atm O_2 pressure, at which Pr
CoO_3 + CoO or $PrCoO_3$ + Pr_6O_{11} are stable
depending upon the total composition of
the samples.

As shown in Fig. 1 abrupt weight changes
take place at values of $-\log P_{O_2}$ of 9.30,
5.73, 3.60, 3.10, 3.05, and 2.05. These val-
ues reflect the oxygen partial pressures at
which three solid phases are in equilibrium.
Among these values, $\log P_{O_2} = -9.30$ corre-
sponds to the oxygen partial pressure of a
reaction, Co + $\frac{1}{2}O_2$ = CoO (1).

The identification of phase was carried
out on samples which were quenched at dif-
ferent conditions of the oxygen partial pres-
sure. Part of the results are shown in Table
I as the two-phase combinations.

Based upon the thermogravimetric
results and the phase identification, the
phase diagram was constructed with apices
of Pr_2O_3, Co, and Co_2O_3 as shown in Fig. 2.
Numerical values in the three solid fields in
Fig. 2 indicate the six equilibrium oxygen

partial pressures as $-\log P_{O_2}$ described
above. Dotted lines represent the isooxy-
gen partial pressures of the two-phase fields
and solid lines are phase boundaries. Seven
phases, Pr_2O_3(R), Pr_6O_{11}, Co, "Pr_2CoO_4"
(A), $Pr_4Co_3O_{10}$(B), $PrCoO_3$(C), and CoO(D)
are stable in the system. At 1200°C Pr_2O_3 is
stable in the oxygen partial pressure range
lower than $\log P_{O_2} = -0.74 \pm 0.05$. Pr_6O_{11} is
not shown in Fig. 2 to avoid confusion.
Co_2O_3 and Co_3O_4 are not found. $PrCoO_3$,
$Pr_4Co_3O_{10}$, and "Pr_2CoO_4" have nonstoi-
chiometric compositions. "Pr_2CoO_4" does
not mean stoichiometric Pr_2CoO_4 which is
indicated by an open circle, A, in Fig. 2.
Here, the quotation marks represent the
component of the phase as well as wüstite
which is indicated by "FeO." The X-ray
powder pattern of "Pr_2CoO_4" which was
made at $\log P_{O_2} = -3.30$ and -5.00 is simi-
lar to that of Kniga et al. (7). They indexed
the structure of Pr_2CoO_4 as tetragonal but
Flamand and Berjoan (4) indexed it as

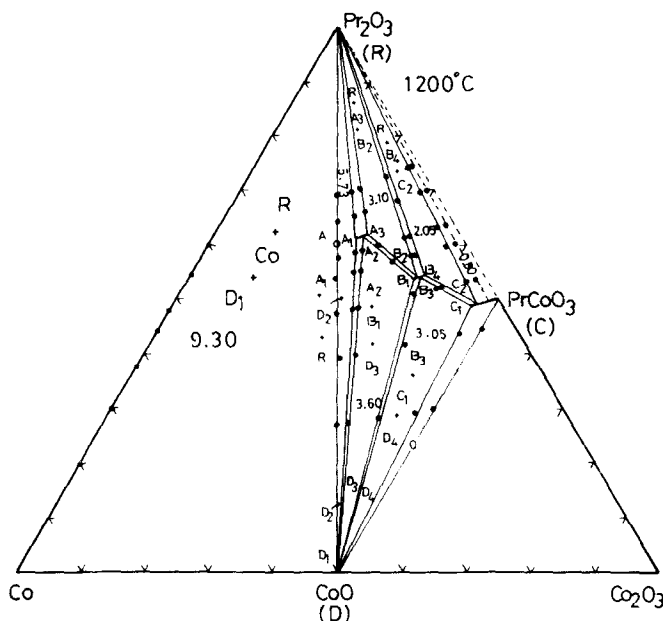

FIG. 2. Phase equilibria in the Pr_2O_3–Co–Co_2O_3 system at 1200°C. Numerical values in three- and
two-phase regions are the oxygen partial pressures in $-\log(P_{O_2}/\text{atm})$ in equilibrium. Symbols are the
same as those in Table III.

TABLE I

IDENTIFICATION OF PHASE

Composition (mole%)		$-\log P_{O_2}$ (atm)	Time (hr)	Phase	
Pr_2O_3	CoO				
60	40	10.00	7	Pr_2O_3	+ Co
		9.00	17	Pr_2O_3	+ CoO
		5.00	30	Pr_2O_3	+ "Pr_2CoO_4"
		2.50	20	Pr_2O_3	+ $Pr_4Co_3O_{10}$
		1.50	24	Pr_2O_3	+ $PrCoO_3$
		0.68	8	Pr_6O_{11}[a]	+ $PrCoO_3$
44	56	5.00	30	"Pr_2CoO_4"	+ CoO
		3.30	23	"Pr_2CoO_4"	+ $Pr_4Co_3O_{10}$
37.5	62.5	3.30	23	CoO	+ $Pr_4Co_3O_{10}$
		2.50	20	$PrCoO_3$	+ $Pr_4Co_3O_{10}$
20	80	5.00	30	CoO	+ "Pr_2CoO_4"
		2.50	20	CoO	+ $PrCoO_3$
		0.68	8	CoO	+ $PrCoO_3$
Eu_2O_3	CoO				
60	40	10.00	6	Eu_2O_3	+ Co
		9.00	8	Eu_2O_3	+ CoO
		2.00	20	Eu_2O_3	+ CoO
		0.68	43	Eu_2O_3	+ $EuCoO_3$
40	60	2.00	20	Eu_2O_3	+ CoO
		0.68	43	$EuCoO_3$	+ CoO
20	80	2.00	20	$EuCoO_3$	+ CoO
Sm_2O_3	CoO				
63	37	10.00	14	Sm_2O_3	+ Co
		9.00	14.5	Sm_2O_3	+ CoO
		0.68	8	Sm_2O_3	+ $SmCoO_3$
30	70	10.00	14	Sm_2O_3	+ Co
		9.00	14.5	Sm_2O_3	+ CoO
		0.68	8	$SmCoO_3$	+ CoO
Tb_2O_3	CoO				
60	40	10.00	8	Tb_2O_3	+ Co
		9.00	8	Tb_2O_3	+ CoO
		2.00	15	Tb_2O_3	+ CoO
		0.68	44	Tb_2O_3	+ CoO
		0	14	Tb_4O_7	+ $TbCoO_3$
25	75	10.00	8	Tb_2O_3	+ Co
		9.00	8	Tb_2O_3	+ CoO
		0.68	44	Tb_2O_3	+ CoO
		0	14	$TbCoO_3$	+ CoO

[a] This phase is not represented in Fig. 2.

TABLE II
Lattice Constants of the Compounds

Compound	−log P_{O_2} (atm)	Other phases	a (Å)	b (Å)	c (Å)	V (Å³)	Ref.
$Pr_4Co_3O_{10}$	3.30	"Pr_2CoO_4"	5.376 ± 0.002	5.458 ± 0.002	27.34 ± 0.02	802.3 ± 0.7	Present
	3.30	CoO	5.377 ± 0.002	5.459 ± 0.002	27.34 ± 0.02	802.7 ± 0.6	Present
			5.390 ± 0.005		27.36 ± 0.04		(8)
"Pr_2CoO_4"	3.30	$Pr_4Co_3O_{10}$	3.878 ± 0.007		12.24 ± 0.05	184.2 ± 1.0	Present
	3.30	Pr_2O_3	3.881 ± 0.008		12.27 ± 0.06	184.8 ± 1.2	Present
			3.87 ± 0.01		12.65 ± 0.02		(7)
$PrCoO_3$	1.50	CoO	7.575 ± 0.002			434.6 ± 0.4	Present
	1.50	Pr_2O_3	7.572 ± 0.003			434.2 ± 0.4	Present
			7.572				(19)
			5.344 ± 0.007	5.358 ± 0.007	7.60 ± 0.01		(3)
			5.331	5.373	7.587	212.44	(20)
$SmCoO_3$	0.68	CoO	5.284 ± 0.006	5.343 ± 0.006	7.506 ± 0.006	211.9 ± 0.4	Present
	0.68	Sm_2O_3	5.283 ± 0.005	5.344 ± 0.005	7.502 ± 0.005	211.8 ± 0.03	Present
			5.294 ± 0.002	5.352 ± 0.002	7.504 ± 0.003	212.6 ± 0.2	(5)
$TbCoO_3$	0	Tb_4O_7	5.209 ± 0.011	5.393 ± 0.006	7.409 ± 0.010	208.1 ± 0.6	Present
	0	CoO	5.203 ± 0.008	5.398 ± 0.005	7.408 ± 0.006	207.7 ± 0.4	Present
			5.209 ± 0.002	5.402 ± 0.002	7.425 ± 0.003	208.9 ± 0.2	(5)
$EuCoO_3$	0.68	CoO	5.259 ± 0.001	5.370 ± 0.001	7.481 ± 0.002	211.2 ± 0.1	Present
	0.68	Eu_2O_3	5.258 ± 0.001	5.371 ± 0.001	7.479 ± 0.002	211.2 ± 0.1	Present
			5.261 ± 0.002	5.369 ± 0.002	7.488 ± 0.003	211.5 ± 0.2	(5)

monoclinic. However, they did not mention the nonstoichiometry of Pr_2CoO_4.

The $Pr_4Co_3O_{10}$ with tetragonal structure was prepared at 1100°C under partial O pressure of 10^{-4} atm (8). At 1200°C the compound is stable in the oxygen partial pressure from $10^{-3.60}$ to $10^{-2.05}$ also.

The relationships between the composition and the oxygen partial pressure of the solid solutions are represented with linear equations, $N_O/N_{PrCoO_3} = 0.0152 \log P_{O_2} - 0.030$ for the $PrCoO_3$ solid solution, $N_O/N_{Pr_4Co_3O_{10}} = 0.0907 \log P_{O_2} + 0.186$ for the $Pr_4Co_3O_{10}$ solid solution, and $N_O/N_{Pr_2CoO_4} = 0.0342 \log P_{O_2} + 0.276$ for the Pr_2CoO_4 solid solution. Here, N denotes the mole fraction of the subscripts. Data for the linear equation concerning the CoO solid solution were reported earlier (1).

Lattice constants of the ternary compounds are listed in Table II. The assignment of the indices of $Pr_4Co_3O_{10}$ were attempted with the aid of the orthorhombic data of $La_4Co_3O_{10}$ although Cherepanov et al. (8) indexed them to be the tetragonal structure described above. The volume values seem to be large, but that of $La_4Co_3O_{10}$ is ~800 Å³, also. Judging from the values of $Pr_4Co_3O_{10}$ in Table II, there is no effect by the coexisting phases. Values of $Pr_4Co_3O_{10}$ which were quenched at $\log P_{O_2} = -2.50$ are almost the same as those quenched at $\log P_{O_2} = -3.30$. For Pr_2CoO_4, Kniga et al. (7) and Flamand and Berjoan (4) reported lattice constants with tetragonal and monoclinic systems, respectively. Based upon Kniga's assignment of index, the present values were determined. The errors are still large, but the values are comparable to those of Kniga et al. and coexisting phases do not affect the values of lattice constants. For lattice constants of $PrCoO_3$, two different systems were adopted as shown in Table II. Here, the cubic system was used be-

cause its index data were available. Coexisting phases do not affect the values of lattice constants.

Three types of phase diagrams concerning the Ln–Co–O system were reported (2). According to the classification, the present one seems to belong to the A type, in which three ternary compounds, Ln_2CoO_4, $Ln_4CoO_3O_{10}$, and $LnCoO_3$, are stable. But the present type is different from the A type, that of La_2O_3–Co–Co_2O_3, because the present type has a two-phase field, Pr_2O_3 + CoO. Because of this two-phase region, three-phase solid regions, Pr_2O_3 + CoO + "Pr_2CoO_4" and Pr_2O_3 + CoO + Co–metal, appear, which are not stable in the A type. Therefore, I would like to assign the present one to a new type, type D.

Ln_2O_3–Co–Co_2O_3 ($Ln = Sm, Eu,$ and Tb). In Fig. 3 the relationships between the oxygen partial pressure and the composition are presented for three mixtures represented by the following mole ratios of starting materials: (a) Sm_2O_3/CoO = 6.32/3.68, (b) 4/6, and (c) 3/7 for the Sm system; (a) Eu_2O_3/CoO = 6/4, (b) 4/6, and (c) 2/8 for the Eu system; and (a) Tb_2O_3/CoO = 6/4, (b) 4/6, (c) 2.5/7.5 for the Tb system. The reference weight was also set at log P_{O_2} = -12.00 at which two phases, Ln_2O_3 + Co–metal, are stable. These patterns are very simple. Abrupt weight changes take place at two oxygen partial pressures: one is the common value, log P_{O_2} = -9.30, at which the reaction, Co + $\frac{1}{2}O_2$ = CoO, appears and the others are 1.82 ± 0.05 for the Sm system, 1.42 ± 0.03 for the Eu system, and 0.53 ± 0.07 for the Tb system.

The results of the phase identification of the three systems are tabulated in Table I together with those of the Pr system. The Sm_2O_3–Co–Co_2O_3 system is drawn in Fig. 4 as the representative. The patterns of the other two systems are almost the same provided that the solid solution ranges of the $LnCoO_3$ and the oxygen partial pressure in

equilibrium with three solid phases, Ln_2O_3 + $LnCoO_3$ + CoO, are different as described above.

In Table III the composition of the compounds at representative points, its symbol, the stability of the compounds in log P_{O_2}, and the activities of the components in the solid solutions are tabulated together with those of the Pr system. From these data and Fig. 3, phase diagrams of the other two can be easily deduced by the reader. These phase diagrams belong to the C type (2) in which one ternary compound, $LnCoO_3$, is stable.

$SmCoO_3$ and $EuCoO_3$ have a small range of nonstoichiometry, which is represented by the equations N_O/N_{SmCoO_3} = 0.0110 log P_{O_2} and N_O/N_{EuCoO_3} = 0.0141 log P_{O_2}, while $TbCoO_3$ is stoichiometric.

(2) The Standard Gibbs Energy of Reaction

On the basis of the established phase diagrams, the standard Gibbs energies of reac-

TABLE III

COMPOSITIONS, SYMBOLS, STABILITY RANGES IN OXYGEN PARTIAL PRESSURES, AND ACTIVITIES IN SOLID SOLUTIONS

Component	Composition	Symbol	$-\log P_{O_2}$ (atm)	$\log a_i$
$PrCoO_3$	$PrCoO_{2.92}$	C_1	3.05	0
	$PrCoO_{2.94}$	C_2	2.05	0.0344
	$PrCoO_{2.97}$	C_3	0.80	0.0668
$Pr_4Co_3O_{10}$	$Pr_4Co_3O_{9.86}$	B_1	3.60	0
	$Pr_4Co_3O_{9.90}$	B_2	3.10	0.0295
	$Pr_4Co_3O_{9.91}$	B_3	3.05	0.0318
	$Pr_4Co_3O_{10.0}$	B_4	2.05	0.0544
Pr_2CoO_4	$Pr_2CoO_{4.08}$	A_1	5.73	0
	$Pr_2CoO_{4.15}$	A_2	3.60	-0.124
	$Pr_2CoO_{4.17}$	A_3	3.10	-0.164
$SmCoO_3$	$SmCoO_{2.98}$	C_1'	1.80	0
	$SmCoO_{3.00}$	C_2'	0	-0.0091
$EuCoO_3$	$EuCoO_{2.98}$	C_1''	1.42	0
	$EuCoO_{3.00}$	C_2''	0	-0.0071
$TbCoO_3$	$TbCoO_{3.00}$	C_1'''	0.53–0	0
CoO	$CoO_{0.991}$	D_1	9.30	0
	$CoO_{0.996}$	D_2	5.73	0.0118
	$CoO_{0.998}$	D_3	3.60	0.0152
	$CoO_{0.999}$	D_4	3.05	0.0157
	$CoO_{1.000}$	D_5	1.82	0.0160
	$CoO_{1.001}$		1.42	0.0159
	$CoO_{1.002}$		0.53	0.0153
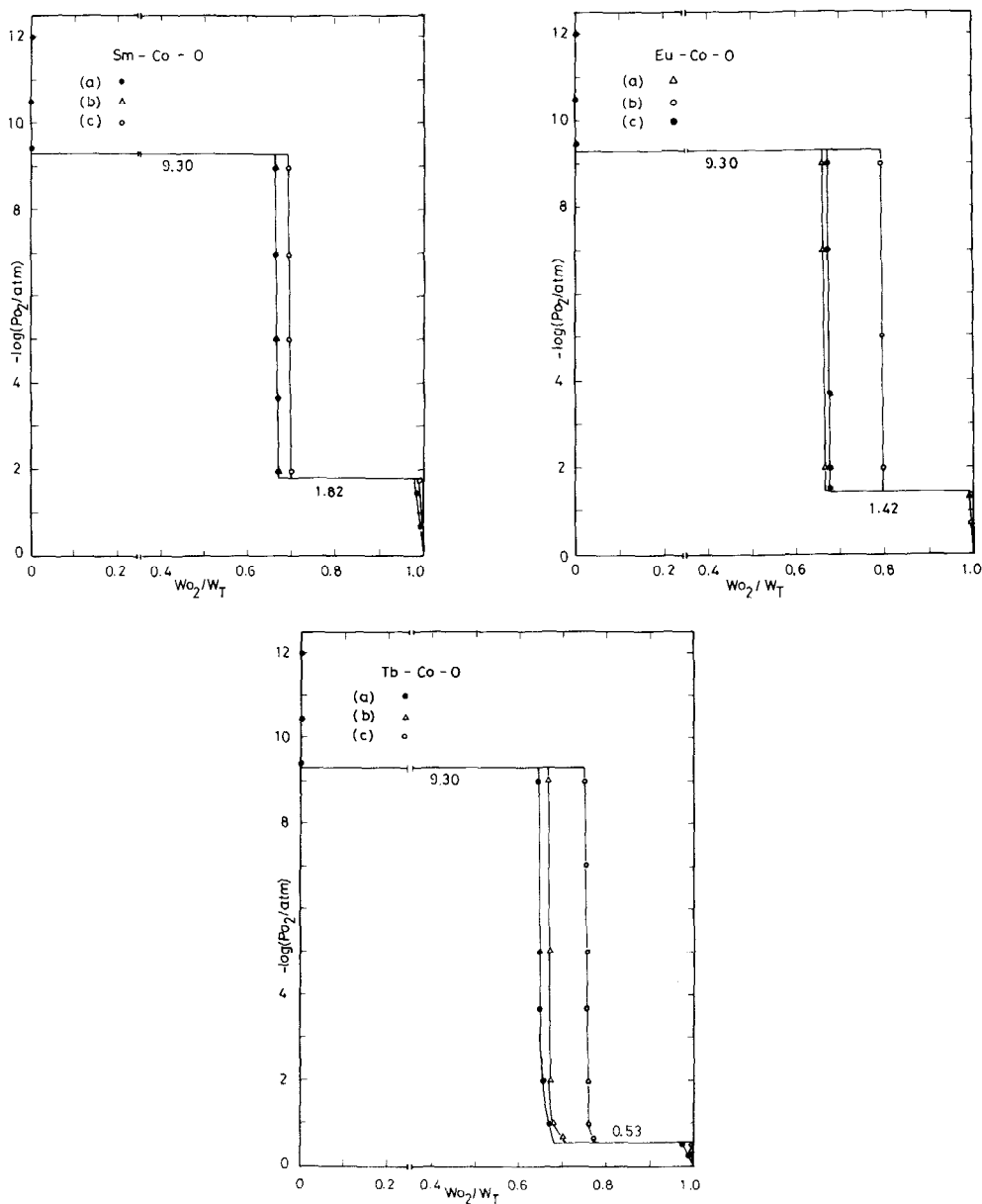
FIG. 3. The relationships between $-\log(P_{O_2}/\text{atm})$ and the weight change, W_{O_2}/W_T, of samples in the Sm, Eu, and Tb systems. The compositions of the starting materials indicated by (a), (b), and (c) are described in the text.

tions, which are given in Table IV, were calculated by the equation, $\Delta G° = -$ RT ln K. The activities in Table III and those of CoO in the CoO solid solution, obtained from previous data (1), were used to calculate K values. By subtracting equation (1) from equation (2), one obtains an equation, $\frac{1}{2}Pr_2O_3 + CoO + \frac{1}{4}O_2 = PrCoO_3$, with $\Delta G°$

FIG. 4. Phase equililbria in the $Sm_2O_3-Co-Co_2O_3$ system at 1200°C. Numerical values in the three-phase regions are the oxygen partial pressures in - $\log(P_{O_2}/atm)$ in equilibrium. Symbols are the same as those in Table III.

= −25.9 kJ. The standard Gibbs energy for the formation of $PrCoO_3$ from common oxides was refined by Petrov et al. (18) and an equation, $\Delta G° = -184,760 + 0.1063 \time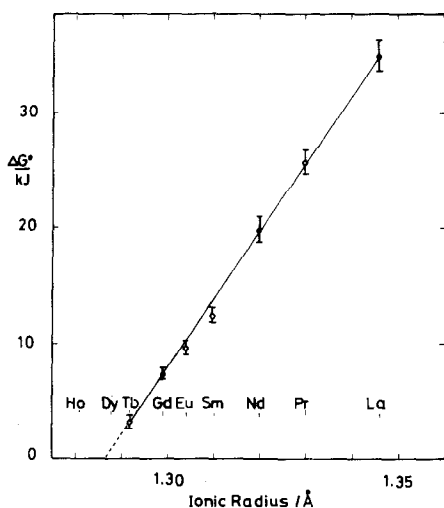s 10^3$ T (J), was obtained. From this equation, the $\Delta G°$ value at 1200°C was calculated to be −28.2 kJ, which is in fairly good agreement with the present one. For reactions (1) × 2 and (2), $\Delta G° \pm 120 = -96,470 + 46.92$ T (K ≤ 1473) and $\Delta G° \pm 140 = -176,350 + 99.55$ T (K ≤ 1473) were presented by Cherepanov et al. (8) using emf measurements, respectively. At 1200°C −13.7 and −29.7 kJ were obtained for both reactions.

TABLE IV

THE GIBBS ENERGY OF REACTIONS

Reaction	$-\log P_{O_2}$ (atm)	$-\Delta G°$ (kJ)	$-\Delta G^{∞}$ (kJ)
(1) $Pr_4Co_3O_{10} + \frac{1}{2}O_2 = \frac{1}{2}Pr_2O_3 + 3PrCoO_3$	2.05 ± 0.03	15.8 ± 0.2	13.7
(2) $Pr_4Co_3O_{10} + CoO + \frac{1}{2}O_2 = 4PrCoO_3$	3.05 ± 0.03	41.7 ± 0.8	29.7
(3) $3Pr_2CoO_4 + \frac{1}{2}O_2 = Pr_4Co_3O_{10} + Pr_2O_3$	3.10 ± 0.03	58.4 ± 0.5	
(4) $2Pr_2CoO_4 + CoO + \frac{1}{2}O_2 = Pr_4Co_3O_{10}$	3.60 ± 0.03	57.3 ± 0.6	
(5) $Pr_2O_3 + CoO + 0.04O_2 = Pr_2CoO_{4.08}$	5.73 ± 0.06	6.1 ± 0.1	
(6) $\frac{1}{2}Sm_2O_3 + CoO + \frac{1}{4}O_2 = SmCoO_3$	1.82 ± 0.05	12.4 ± 0.5	
(7) $\frac{1}{2}Eu_2O_3 + CoO + \frac{1}{4}O_2 = EuCoO_3$	1.42 ± 0.03	9.6 ± 0.5	
(8) $\frac{1}{2}Tb_2O_3 + CoO + \frac{1}{4}O_2 = TbCoO_3$	0.53 ± 0.07	3.3 ± 0.5	

[a] Cherepanov et al. (8).

FIG. 5. The relationship between the ionic radius of lanthanoid elements in 12 coordination and $\Delta G°$ values of reaction, $\frac{1}{2}Ln_2O_3$ + CoO + $\frac{1}{4}O_2$ = $LnCoO_3$.

The latter value is higher than the present value, but the reason for the difference is not yet clear.

(3) The Relationship between $\Delta G°$ and Ionic Radius

In the previous report (2), the Gibbs energy of the reaction, $\frac{1}{2}Ln_2O_3$ + CoO + $\frac{1}{4}O_2$ = $LnCoO_3$, showed a linear change with the ionic radius of lanthanoid elements with 12 coordination. It is of interest whether or not the present three values fit on the previous linear line. In Fig. 5 these values were plotted with open circles together with the previous three. They fit well. The values for $LaCoO_3$ and $PrCoO_3$ fit especially well despite the difference of the crystal system

from other perovskite structures. This implies that the crystal system has a smaller effect on $\Delta G°$ than the ionic radius.

References

1. K. KITAYAMA, *J. Solid State Chem.* **73**, 381 (1988).
2. K. KITAYAMA, *J. Solid State Chem.*, in press.
3. S. A. NEDIL'KO, M. N. ERMAKOVA, L. D. LYASHKO, AND S. M. GOZHDZINSKII, *Zh. Neorg. Khim.* **24**, 1395 (1979).
4. R. FLAMAND AND R. BERJOAN, *High Temp.-High Pressures* **15**, 693 (1983).
5. G. DEMAZEAU, M. POUCHARD, AND P. HAGENMULLER, *J. Solid State Chem.* **9**, 202 (1974).
6. U. LEHMANN AND HK. MÜLLER-BUSCHBAUM, *Z. Anorg. Allg. Chem.* **470**, 59 (1980).
7. M. V. KNIGA, I. I. VYGOUSKII, AND E. E. KLEMENTOVICH, *Zh. Neorg. Khim.* **24**, 1171 (1979).
8. V. A. CHEREPANOV, A. N. PETROV, AND L. YU. GRIMOVA, *Zh. Fiz. Khim.* **59**, 2131 (1985).
9. A. YU. KROPANOV, A. N. PETROV, AND V. M. ZHUKOVSKII, *Zh. Neorg. Khim.* **28**, 2938 (1983).
10. T. KATSURA, K. KITAYAMA, T. SUGIHARA, AND N. KIMIZUKA, *Bull. Chem. Soc. Japan* **48**, 1809 (1975).
11. K. KITAYAMA AND T. KATSURA, *Bull. Chem. Soc. Japan* **58**, 948 (1985).
12. T. SUGIHARA, Thesis, Tokyo Institute of Technology (1978).
13. JCPDS Card, No. 6-410.
14. JCPDS Card, No. 23-1418.
15. N. KIMIZUKA AND T. KATSURA, *J. Solid State Chem.* **13**, 176 (1975).
16. T. KATSURA AND A. MUAN, *Trans. Amer. Inst. Min., Metall. Pet. Eng.* **230**, 77 (1964).
17. T. KATSURA AND H. HASEGAWA, *Bull. Chem. Soc. Japan* **40**, 561 (1967).
18. A. N. PETROV, V. A. CHEREPANOV, AND A. YU. ZUEV, *Zh. Fiz. Khim.* **61**, 630 (1987).
19. JCPDS Card, No. 25-1068.
20. A. KAPPATSCH, S. QUEZEL-AMBRUNAZ, AND J. SIVARDIÉRE, *J. Phys.* **31**, 369 (1970).